J|A|C|S
ARTICLES
Published on Web 01/03/2002

pH-Dependent H_2-Activation Cycle Coupled to Reduction of Nitrate Ion by Cp*Ir Complexes

Seiji Ogo,*,† Hidetaka Nakai,† and Yoshihito Watanabe*,†,‡

Contribution from the Institute for Molecular Science, Myodaiji, Okazaki 444-8585, Japan, and Center for Integrative Bioscience, Myodaiji, Okazaki 444-8585, Japan

Received July 30, 2001

Abstract: This paper reports a pH-dependent H_2-activation {H_2 (pH 1−4) → $H^+ + H^-$ (pH −1) → $2H^+ + 2e^-$} promoted by Cp*Ir complexes {Cp* = η^5-$C_5(CH_3)_5$}. In a pH range of about 1−4, an aqueous HNO_3 solution of $[Cp^*Ir^{III}(H_2O)_3]^{2+}$ (**1**) reacts with 3 equiv of H_2 to yield a solution of $[(Cp^*Ir^{III})_2(\mu\text{-}H)_3]^+$ (**2**) as a result of heterolytic H_2-activation {2[**1**] + $3H_2$ (pH 1−4) → [**2**] + $3H^+ + 6H_2O$}. The hydrido ligands of **2** display protonic behavior and undergo H/D exchange with D^+: $[M-(H)_3-M]^+ + 3D^+ \rightleftharpoons [M-(D)_3-M]^+ + 3H^+$ (where M = Cp*Ir). Complex **2** is insoluble in a pH range of about −0.2 (1.6 M HNO_3/H_2O) to −0.8 (6.3 M HNO_3/H_2O). At pH −1 (10 M HNO_3/H_2O), a powder of **2** drastically reacts with HNO_3 to give a solution of $[Cp^*Ir^{III}(NO_3)_2]$ (**3**) with evolution of H_2, NO, and NO_2 gases. D-labeling experiments show that the evolved H_2 is derived from the hydrido ligands of **2**. These results suggest that oxidation of the hydrido ligands of **2** {[**2**] + $4NO_3^-$ (pH −1) → 2[**3**] + $H_2 + H^+ + 4e^-$} couples to reduction of NO_3^- ($NO_3^- \rightarrow NO_2^- \rightarrow NO$). To complete the reaction cycle, complex **3** is transformed into **1** by increasing the pH of the solution from −1 to 1. Therefore, we are able to repeat the reaction cycle using **1**, H_2, and a pH gradient between 1 and −1. A conceivable mechanism for the H_2-activation cycle with reduction of NO_3^- is proposed.

Introduction

The chemistry of water-soluble organometallic complexes is presently undergoing very rapid growth because of many potential advantages such as alleviation of environmental problems associated with the use of organic solvents, industrial applications (e.g., introduction of new biphasic processes), and reaction-specific pH selectivity.[1] pH-dependent H_2-activation in aqueous media is one of the applications of the water-soluble organometallic complexes.[2] Herein, we report a unique pH-dependent H_2-activation cycle coupled to the reduction of the nitrate ion (NO_3^-). As shown in Scheme 1, the cycle is promoted by an aqua complex $[Cp^*Ir^{III}(H_2O)_3]^{2+}$ {**1**, Cp* = η^5-$C_5(CH_3)_5$},[3] a well-known dinuclear trihydrido complex $[(Cp^*Ir^{III})_2(\mu\text{-}H)_3]^+$ (**2**),[4] and a nitrato complex $[Cp^*Ir^{III}(NO_3)_2]$ (**3**) in a pH range of 4 to −1. To determine the structures of **2** and **3** in these acidic media, crystals obtained from 0.1 M HNO_3/H_2O (pH 1)

Scheme 1

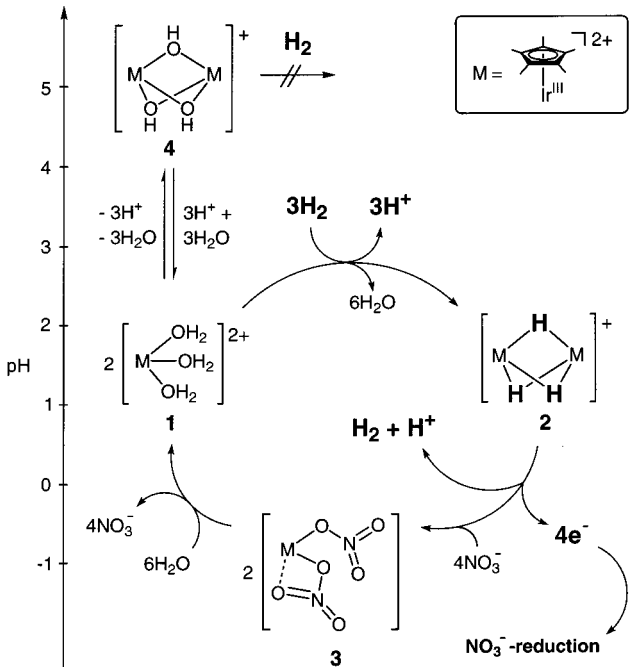

* To whom correspondence should be addressed.
† Institute for Molecular Science.
‡ Center for Integrative Bioscience.

(1) (a) Cornils, B.; Herrmann, W. A. *Aqueous-Phase Organometallic Catalysis*; Wiley−VCH: Weinheim, 1998; p 615. (b) Li, C.-J.; Chan, T.-H. *Organic Reactions in Aqueous Media*; John Wiley & Sons: New York, 1997; p 199. (c) Horváth, I. T.; Joó, F. *Aqueous Organometallic Chemistry and Catalysis*; Kluwer Academic Publishers: Dordrecht, 1995; p 317. (d) Fish, R. H. *Coord. Chem. Rev.* **1999**, *185/186*, 569−584. (e) Joó, F.; Kathó, A. *J. Mol. Catal. A* **1997**, *116*, 3−26. (f) Koelle, U. *Coord. Chem. Rev.* **1994**, *135/136*, 623−650. (g) Herrmann, W. A.; Kohlpaintner, C. W. *Angew. Chem., Int. Ed. Engl.* **1993**, *32*, 1524−1544.

(2) (a) Makihara, N.; Ogo, S.; Watanabe, Y. *Organometallics* **2001**, *20*, 497−500. (b) Joó, F.; Kovács, J.; Bényei, A. C.; Nádasdi, L.; Laurenczy, G. *Chem.-Eur. J.* **2001**, *7*, 193−199. (c) Kovács, J.; Todd, T. D.; Reibenspies, J. H.; Joó, F.; Darensbourg, D. J. *Organometallics* **2000**, *19*, 3963−3969. (d) Tin, K.-C.; Wong, N.-B.; Li, R.-X.; Li, Y.-Z.; Hu, J.-Y.; Li, X.-J. *J. Mol. Catal. A* **1999**, *137*, 121−125. (e) Joó, F.; Kovács, J.; Bényei, A. C.; Kathó, Á. *Angew. Chem., Int. Ed.* **1998**, *37*, 969−970. (f) Paterniti, D. P.; Roman, P. J., Jr.; Atwood, J. D. *Organometallics* **1997**, *16*, 3371−3376.

(3) (a) Ogo, S.; Makihara, N.; Watanabe, Y. *Organometallics* **1999**, *18*, 5470−5474. (b) Dadci, L.; Elias, H.; Frey, U.; Hörnig, A.; Koelle, U.; Merbach, A. E.; Paulus, H.; Schneider, J. S. *Inorg. Chem.* **1995**, *34*, 306−315.

(4) White, C.; Oliver, A. J.; Maitlis, P. M. *J. Chem. Soc., Dalton Trans.* **1973**, 1901−1907.

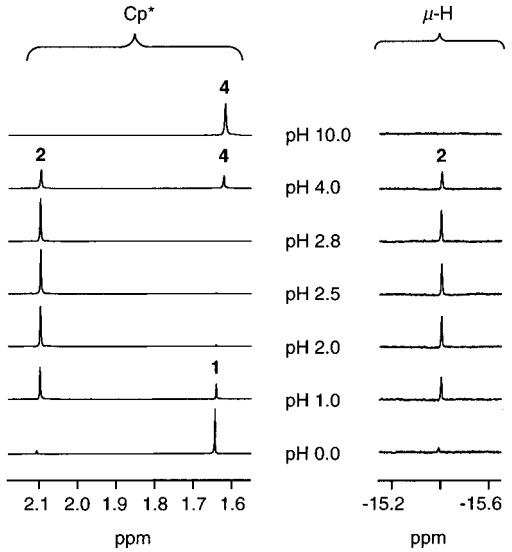

Figure 1. pH-dependent ^{1}H NMR spectra of the reaction of **1** (10 μmol) with H_2 (0.1 MPa) in HNO_3/H_2O (1 mL) for 1 h at 30 °C.

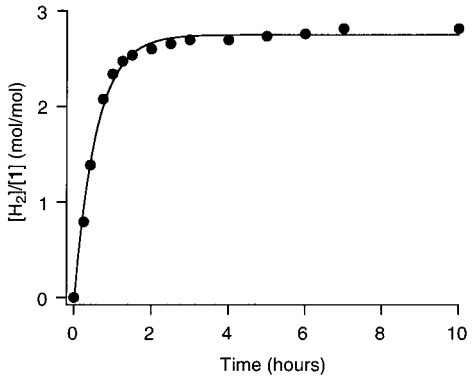

Figure 2. Time course of H_2-consumption on the reaction of **1** (100 μmol) with H_2 (0.1 MPa) in HNO_3/H_2O (10 mL) at pH 2 at 30 °C to yield **2** monitored by a constant pressure gas buret.

solutions of **2** and 10 M HNO_3/H_2O (pH −1) solutions of **3** were used for X-ray analysis. Furthermore, electrospray ionization mass spectrometry (ESI-MS) experiments of **2** and **3** were also carried out under these acidic conditions.

Results and Discussions

Heterolytic H_2-Activation. The aqua complex $[Cp^*Ir^{III}(H_2O)_3]$-SO_4 (**1**·SO_4) was prepared by the method described in a previous paper.[3a] In a pH range of about 1−4, a pale-yellow solution of **1** reacts with H_2 quantitatively (3 equiv of H_2 based on **1**) to yield a yellow solution of **2** as a result of heterolytic H_2-activation {2[**1**] + $3H_2$ (pH 1−4) → [**2**] + $3H^+$ + $6H_2O$}. Figure 1 shows pH-dependent ^{1}H NMR spectra of the reaction of **1** (10 μmol) with H_2 (0.1 MPa) in aqueous HNO_3 (1 mL) for 1 h at 30 °C. The time course of H_2-consumption on the reaction of **1** (100 μmol) with H_2 (0.1 MPa) in aqueous HNO_3 (10 mL) at pH 2 at 30 °C was measured by a constant pressure gas buret (Figure 2). With the progress of the reaction, the pH of the solution is decreased because of the heterolytic H_2-activation giving protons and **2**. We propose that the H_2O ligands in **1** could act as a base to release H_3O^+ ($H_2 + H_2O \rightarrow H^- + H_3O^+$) and accelerate the heterolytic H_2-activation to form **2** under these conditions since it has been known that polar solvents accelerate the heterolytic activation of H_2.[5] In addition,

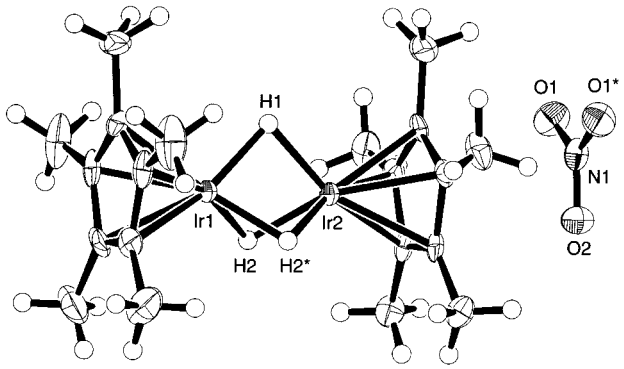

Figure 3. ORTEP drawing of **2**·NO_3. Crystals of **2**·NO_3 were obtained from a 0.1 M HNO_3/H_2O (pH 1) solution of **2**. Selected bond lengths (Å) and angles (deg): Ir1−H1 = 1.75(10), Ir1−H2 = 1.78(6), Ir2−H1 = 1.79(9), Ir2−H2 = 1.76(6); Ir1−H1−Ir2 = 88(4), Ir1−H2−Ir2 = 89(3).

above pH 4, complex **1** is reversibly deprotonated to form a dinuclear trihydroxo complex $[(Cp^*Ir^{III})_2(\mu\text{-}OH)_3]^+$ (**4**)[6] that does not react with H_2 under these conditions (Scheme 1 and Figure 1).

Characterization of 2 in the Acidic Media. Hydrogen atoms attached to transition metals are hydrides, and the hydridic behavior can be accessed by appropriate reagents. The release of the hydrogen atom as a proton can also be invoked by appropriate reagents. It is thus of interest to investigate the structures and properties of these transition metal hydrides, especially, having the ligands of cyclopentadienyl derivatives, such as $[(Cp^*Fe^{III})_2(\mu\text{-}H)_4]$ and $[(Cp^*Ir^{II})_2(\mu\text{-}H)_2]$.[7] The structure of **2** in the acidic media (pH 1−4) was determined by ^{1}H NMR (Figure 1), X-ray analysis, and ESI-MS. Crystals of **2**·NO_3 used in the X-ray analysis (Figure 3)[8] were obtained from a 0.1 M HNO_3/H_2O (pH 1) solution of **2**. The bonding parameters of **2**·NO_3 are very close to those of **2**·ClO_4 previously determined by X-ray and neutron diffraction structure analysis.[9] The Ir···Ir distances of **2**·NO_3 and **2**·ClO_4 are 2.4677(4) and 2.465(3) Å, respectively.

Above pH 1, complex **2** is soluble in HNO_3/H_2O at 30 °C. The positive-ion ESI mass spectrum of **2** in 0.1 M HNO_3/H_2O (pH 1) shows the consistency with a formulation or the binuclearity; that is, a prominent signal at *m*/*z* 657.4 {relative intensity (*I*) = 100% in the range of *m*/*z* 100−2000, Figure 4a} has a characteristic distribution of isotopomers (Figure 4b) that matches well with the calculated isotopic distribution for $[(Cp^*Ir^{III})_2(\mu\text{-}H)_3]^+$ ([**2**]$^+$, Figure 4c). To establish the origin of the hydrido ligands of **2**, the synthesis of D-labeled **2** {$[(Cp^*Ir^{III})_2(\mu\text{-}D)_3]^+$} by a reaction of **1** (10 μmol) with D_2 (0.1 MPa) in HNO_3/H_2O (1 mL) at pH 2 for 15 min at 30 °C has been carried out. ESI-MS results show that the signal at *m*/*z* 657.4 shifts to *m*/*z* 660.4 {$[(Cp^*Ir^{III})_2(\mu\text{-}D)_3]^+$}. This indicates that the deuterium atoms are incorporated in **2** (Figure 4d−f) and the rate of the H/D exchange between the bridging deuterido

(5) Brothers, P. J. *Prog. Inorg. Chem.* **1981**, *28*, 1−61.
(6) Nutton, A.; Bailey, P. M.; Maitlis, P. M. *J. Chem. Soc., Dalton Trans.* **1981**, 1997−2002.
(7) (a) Ohki, Y.; Suzuki, H. *Angew. Chem., Int. Ed.* **2000**, *39*, 3120−3122. (b) Hou, Z.; Koizumi, T.; Fujita, A.; Yamazaki, H.; Wakatsuki, Y. *J. Am. Chem. Soc.* **2001**, *123*, 5812−5813.
(8) Crystal data for **2**·$(NO_3)(H_2O)_4$: $C_{20}H_{41}Ir_2NO_7$, MW 791.99, monoclinic, space group $P2_1/m$ (No. 11), a = 7.330(3) Å, b = 13.480(6) Å, c = 13.190(1) Å, β = 101.890(2)°, V = 1275.3(8) Å^3, Z = 2, D_c = 2.062 g cm^{-3}, μ(Mo Kα) = 104.90 cm^{-1}, R = 0.034, and R_w = 0.095.
(9) Stevens, R. C.; Mclean, M. R.; Wen, T.; Carpenter, J. D.; Bau, R.; Koetzle, T. F. *Inorg. Chim. Acta* **1989**, *161*, 223−231.

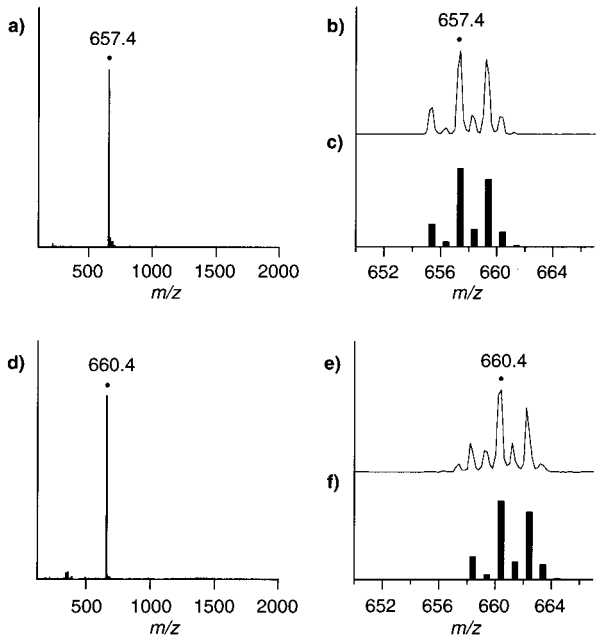

Figure 4. (a) Positive-ion ESI mass spectrum of **2** in 0.1 M HNO_3/H_2O (pH 1). The signal at *m*/*z* 657.4 corresponds to $[\mathbf{2}]^+$. (b) The signal at *m*/*z* 657.4. (c) Calculated isotopic distribution for $[\mathbf{2}]^+$. (d) Positive-ion ESI mass spectrum of D-labeled **2** prepared by a reaction of **1** (10 μmol) with D_2 (0.1 MPa) in HNO_3/H_2O (1 mL, pH 2) for 15 min at 30 °C. The signal at *m*/*z* 660.4 corresponds to $[(Cp^*Ir^{III})_2D_3]^+$. (e) The signal at *m*/*z* 660.4. (f) Calculated isotopic distribution for $[(Cp^*Ir^{III})_2D_3]^+$.

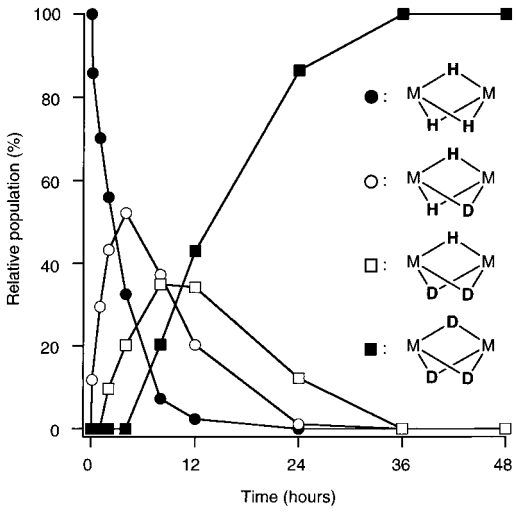

Figure 5. H/D exchange of **2** (5 μmol) with D^+ (0.1 M DNO_3/D_2O, 1 mL, at pD 1.4) at 30 °C monitored by ^{1}H NMR and ESI-MS. M = Cp*Ir.

ligands and H^+ (HNO_3/H_2O) is kinetically slow enough to observe the signal at *m*/*z* 660.4 $\{[(Cp^*Ir^{III})_2(\mu\text{-}D)_3]^+\}$ in HNO_3/H_2O at pH 2.[10] In a pD range of about 1.4−3.4 (pD = pH meter reading + 0.4),[11] complex **2** undergoes the H/D exchange with D^+ (DNO_3/D_2O): $[M-(H)_3-M]^+ + 3D^+ \rightleftharpoons [M-(D)_3-M]^+ + 3H^+$ through $[M-(H)_2(D)-M]^+$ and $[M-(H)(D)_2-M]^+$ species (Figure 5, where M = Cp*Ir, at pD 1.4).[12] In the pD range, the more pD of the solution is low, the more the rate of the H/D exchange is fast. This suggests that the rate of the H/D exchange is dependent on the D^+ concentration or the counterion (NO_3^- as a conjugate base) concentration.[13]

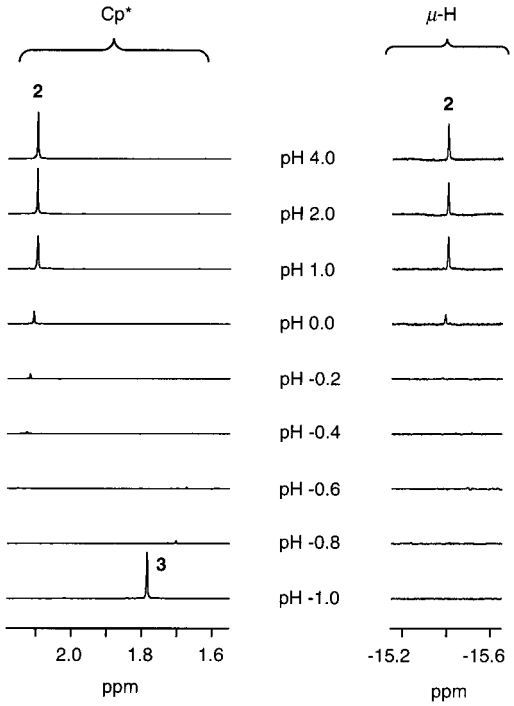

Figure 6. pH-dependent ^{1}H NMR spectra changes of **2** (10 μmol) in HNO_3/H_2O (1 mL) from pH 4 to −1 at 30 °C. In a pH range of about −0.2 (1.6 M HNO_3/H_2O) to −0.8 (6.3 M HNO_3/H_2O), complex **2** is insoluble. At pH −1 (10 M HNO_3/H_2O), a powder of **2** drastically reacts with HNO_3 to give a solution of **3**.

Oxidation of the Hydrido Ligands of 2 Coupled to Reduction of NO_3^-. Figure 6 shows pH-dependent ^{1}H NMR spectra changes of **2** from pH 4 to −1 at 30 °C. In a pH range of about −0.2 (1.6 M HNO_3/H_2O) to −0.8 (6.3 M HNO_3/H_2O), complex **2** is insoluble because of the common ion effect of NO_3^-, and it was confirmed that complex **2** shows similar solubility toward the aqueous solution of $NaNO_3$. At pH −1 (10 M HNO_3/H_2O), a yellow powder of **2** drastically reacts with HNO_3 to give a pale-yellow solution of **3** with evolution of H_2, nitrogen monoxide (NO), and nitrogen dioxide (NO_2) gases (Figure 7). The evolved NO and NO_2 gases were determined by an NO_x gas analyzer. To establish the origin of the evolved H_2, the reaction of **2** with 10 M DNO_3/D_2O has been carried out. Intriguingly, gas chromatographic (GC) experiments show that the evolved gas is H_2 but not HD or D_2. Alternatively, the reaction of D-labeled **2** $\{[(Cp^*Ir^{III})_2(\mu\text{-}D)_3]^+\}$ with 10 M HNO_3/H_2O provides only D_2 but not HD or H_2. Thus, the evolved H_2 (or D_2) is derived from the hydrido ligands of **2** (or D-labeled **2**). We propose that below pD 0.4, the powder of **2** does not undergo the H/D exchange with D^+ (DNO_3/D_2O) before the intramolecular H_2-formation, though above pD 1.4, complex **2** is soluble in DNO_3/D_2O and undergoes the H/D exchange with D^+. These results suggest that at pH −1, oxidation of the hydrido ligands of **2** $\{[\mathbf{2}] + 4NO_3^-$ (pH −1) → $2[\mathbf{3}] + H_2 + H^+ + 4e^-\}$ couples to reduction of NO_3^- ($NO_3^- \rightarrow NO_2^- \rightarrow$ NO). It is important to note that the transformation of **2** to **3** does not occur in saturated (ca. 10 M) $NaNO_3/H_2O$.

(10) (a) Ovchinnikov, M. V.; Angelici, R. J. *J. Am. Chem. Soc.* **2000**, *122*, 6130−6131. (b) Ovchinnikov, M. V.; Guzei, I. A.; Angelici, R. J. *Organometallics* **2001**, *20*, 691−696.
(11) Glasoe, P. K.; Long, F. A. *J. Phys. Chem.* **1960**, *64*, 188−190.
(12) Similarly the isotope exchange from $[M-(D)_3-M]^+$ to $[M-(H)_3-M]^+$ occurs in a pH range of about 1 to 3.
(13) Darensburg and Ludving have described a counterion carrier effect to reduce the kinetic barrier for proton extraction from a metal hydride. Darensbourg, M. Y.; Ludving, M. M. *Inorg. Chem.* **1986**, *25*, 2894−2898.

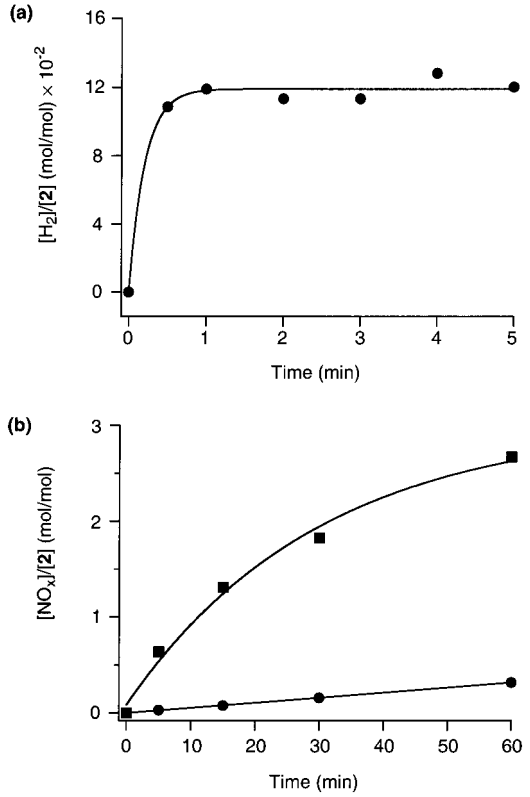

Figure 7. (a) Time course of H_2-evolution of the reaction of **2** (7.2 mg, 10 μmol) with 10 M HNO_3/H_2O (1 mL, pH −1) at 30 °C monitored by GC. (b) Time course of evolution of NO (●) and NO_2 (■) of the reaction of **2** (7.2 mg, 10 μmol) with 10 M HNO_3/H_2O (1 mL, pH −1) at 30 °C monitored by an NO_x gas analyzer.

Scheme 2†

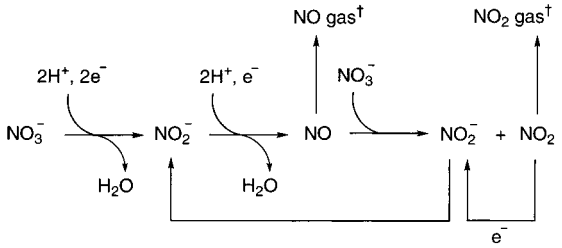

† Evolved NO and NO_2 gases were determined by an NO_x gas analyzer.

Mechanism for the Reduction of NO_3^-. The reduction of nitrate ion (NO_3^-) is of interest as a means of mimicking reduction processes of oxido-nitrogen substrates in nature.[14] We propose a mechanism for the reduction of NO_3^- as follows. At pH −1, one hydrido ligand of **2** behaves as H^+ and reacts with another hydrido ligand (H^-) of **2** to evolve H_2. Eventually, electrons from **2** are utilized for the reduction of NO_3^- into NO_2^- (nitrite ion). It appears that the evolution of H_2 is a trigger for the reduction of NO_3^- since GC experiments show that only 0.12 equiv (based on **2**) of H_2 is evolved in the early stage (within 30 s) of the NO_3^- reduction (Figure 7a). As shown in Scheme 2, once NO_2^- is formed, NO_2^- is readily reduced into NO with consumption of any Cp*Ir reducing species.[15] Furthermore, under the acidic conditions, NO is oxidized to NO_2 by NO_3^- that is reduced to NO_2^-. Formed NO_2 can be reduced by the Cp*Ir reducing species to regenerate NO_2^-.

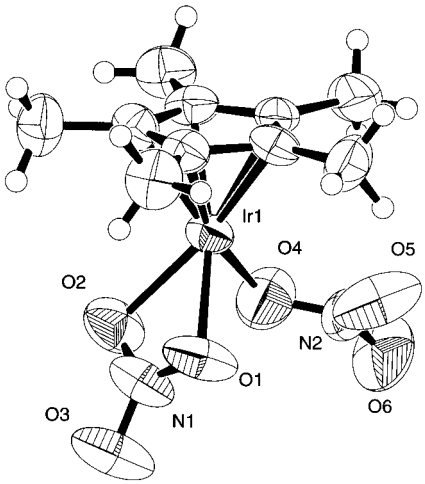

Figure 8. ORTEP drawing of **3**. Crystals of **3** were obtained from a 10 M HNO_3/H_2O solution of **3**. Selected bond lengths (Å) and angles (deg): Ir1−O1 = 2.165(8), Ir1−O2 = 2.184(8), Ir1−O4 = 2.120(9), O1−N1 = 1.25(1), O2−N1 = 1.24(1), O3−N1 = 1.23(1), O4−N2 = 1.29(1), O5−N2 = 1.20(1), O6−N2 = 1.15(1); O1−Ir1−O2 = 57.9(3), O1−Ir1−O4 = 84.2(4), O2−Ir1−O4 = 74.7(4), Ir1−O1−N1 = 93.5(7), Ir1−O2−N1 = 93.0(6), Ir1−O4−N2 = 118.6(8), O1−N1−O2 = 115.2(9), O1−N1−O3 = 121(1), O2−N1−O3 = 122(1), O4−N2−O5 = 113(1), O4−N2−O6 = 125(1), O5−N2−O6 = 119(1).

Characterization of 3 in the Acidic Media. The structure of **3** in 10 M HNO_3/H_2O (pH −1) was determined by ^{1}H NMR (Figure 6), X-ray analysis, and ESI-MS. Crystals of **3** used in the X-ray analysis were obtained from a 10 M HNO_3/H_2O (pH −1) solution of **3**. An ORTEP drawing of **3** is shown in Figure 8.[16] Complex **3** adopts a distorted octahedral geometry with the Ir atom coordinated by one Cp* and two NO_3^- (one monodentate and one bidentate) ligands. Such coordination modes of nitrato ligands in a discrete molecule are also found in $[Cp^*Rh^{III}(NO_3)_2]$.[17] The Ir−O bond length of **3** {2.120(9) and average of 2.175 Å for mono- and bidentate coordination modes, respectively} is close to the Rh−O bond length observed in $[Cp^*Rh^{III}(NO_3)_2]$ {2.135(4) and average of 2.186 Å for the mono- and bidentate coordination modes, respectively}, but is somewhat different from the Ir−O bond length observed in $[Ir^{III}H(NO_3)_2(PPh_3)_2]$ {2.03(4) and average of 2.27 Å for the mono- and bidentate coordination modes, respectively}.[18] The positive-ion ESI mass spectrum of **2** dissolved in 10 M HNO_3/H_2O (pH −1) shows a prominent signal at *m*/*z* 390.2 (I = 100% in the range of *m*/*z* 100−600, Figure 9a), which has a characteristic distribution of isotopomers (Figure 9b) that matches well with the calculated isotopic distribution for $[\mathbf{3} - NO_3]^+$ (Figure 9c).

Conclusions

In summary, the Cp*Ir complexes **1**, **2**, and **3** promote the pH-dependent H_2-activation cycle coupled to reduction of NO_3^-. In the pH range of about 1−4, the solution of **1** reacts with H_2

(14) (a) Tanaka, K.; Komeda, N.; Matsui, T. *Inorg. Chem.* **1991**, *30*, 3282−3288. (b) Willner, I.; Lapidot, N.; Riklin, A. *J. Am. Chem. Soc.* **1989**, *111*, 1883−1884. (c) Moyer, B. A.; Meyer, T. J. *J. Am. Chem. Soc.* **1979**, *101*, 1326−1328.

(15) Fukuzumi, S.; Yorisue, T. *Chem. Lett.* **1991**, 1913−1916.

(16) Crystal data for **3**: $C_{10}H_{15}IrN_2O_6$, MW 451.46, orthorhombic, space group *Pbca* (No. 61), a = 14.893(3) Å, b = 14.413(2) Å, c = 13.068(2) Å, V = 2805(1) Å^3, Z = 8, D_c = 2.138 g cm^{-3}, μ(Mo Kα) = 95.69 cm^{-1}, R = 0.042, and R_w = 0.149.

(17) Hursthouse, M. B.; Malik, K. M. A.; Mingos, D. M. P.; Willoughby, S. D. *J. Organomet. Chem.* **1980**, *192*, 235−251.

(18) Cash, D. N.; Harris, R. O.; Nyburg, S. C.; Pickard, F. H. *J. Cryst. Mol. Struct.* **1975**, *5*, 377−385.

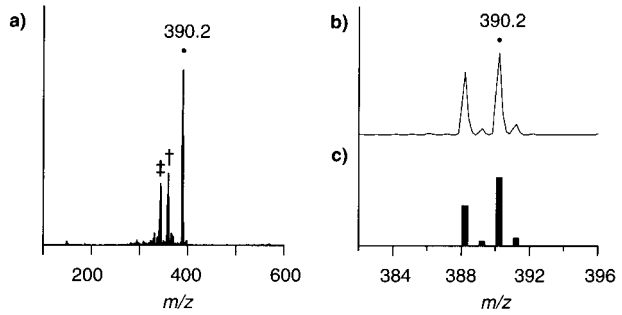

Figure 9. (a) Positive-ion ESI mass spectrum of **2** dissolved in 10 M HNO_3/H_2O (pH −1). The signal at *m*/*z* 390.2 corresponds to $[\mathbf{3} - NO_3]^+$. † (*m*/*z* 360.2) and ‡ (*m*/*z* 344.2) are product ions of $[\mathbf{3} - NO_3]^+$ and correspond to $[\mathbf{3} - NO_3 - NO]^+$ and $[\mathbf{3} - NO_3 - NO_2]^+$, respectively. (b) The signal at *m*/*z* 390.2. (c) Calculated isotopic distribution for $[\mathbf{3} - NO_3]^+$.

to yield the solution of **2** as the result of heterolytic H_2-activation $\{2[\mathbf{1}] + 3H_2$ (pH 1−4) → $[\mathbf{2}] + 3H^+ + 6H_2O\}$. Complex **2** is insoluble in the pH range of about −0.2 (1.6 M HNO_3/H_2O) to −0.8 (6.3 M HNO_3/H_2O). At pH −1, the powder of **2** reacts with HNO_3 to give the solution of **3** with oxidation of the hydrido ligands of **2** $\{[\mathbf{2}] + 4NO_3^-$ (pH −1) → $2[\mathbf{3}] + H_2 + H^+ + 4e^-\}$ and reduction of NO_3^- (NO_3^- → NO_2^- → NO). The unique reactivity of **2** is governed by the bridging hydrido ligands which display protonic behavior and undergo H/D exchange with D^+. To complete the reaction cycle, complex **3** is transformed into **1** by increasing the pH of the aqueous HNO_3 solution from −1 to 1 (Scheme 1). Finally, it was confirmed that the reaction cycle can be repeated at least three times by using **1**, H_2, and a pH gradient between 1 and −1.

Experimental Section

Materials and Methods. All experiments were carried out under an Ar (or N_2) atmosphere by using standard vacuum line techniques or a glovebox. The manipulations in the acidic media were carried out with plastic- and glasswares (without metals). The 65% HNO_3/H_2O (for ultratrace analysis) was purchased from Wako Pure Chemical Industries, Ltd., 65% DNO_3/D_2O (99% D) was purchased from Isotec Inc., and D_2O (99.9% D) was purchased from Cambridge Isotope Laboratories, Inc.; these reagents were used as received. Purification of water (18.2 MΩ cm) was performed with a Milli-Q system (Millipore; Milli-RO 5 plus and -Q plus). H_2 gas (>99.9999%) was purchased from Taiyo Toyo Sanso Co., Ltd., D_2 gas (>99.5%) was purchased from Sumitomo Seika Chemicals Co., Ltd., and HD gas (HD 97%, H_2 1.8%, D_2 1.2%) was purchased from Isotec Inc.; these were used without further purification. NO gas (>99%) was purchased from Nippon Sanso Co. and purified by passing through a saturated NaOH solution to remove NO_2.

The ^1H and ^{13}C NMR spectra were recorded on a JEOL JNM-LA 500 spectrometer at 30 °C. To determine the exact pH values, the NMR experiments were performed by dissolving the samples in HNO_3/H_2O in an NMR tube (diameter = 5.0 mm) with a sealed capillary tube (diameter = 1.5 mm) containing 3-(trimethylsilyl)propionic-2,2,3,3-d_4 acid sodium salt (TSP; 500 mM) dissolved in D_2O (for deuterium lock). ESI-MS data were obtained by an API 300 triple quadrupole mass spectrometer (PE-Sciex) in positive detection mode, equipped with an ion spray interface. The sprayer was held at a potential of 4.5 kV, and compressed N_2 was employed to assist liquid nebulization. Orifice potential was maintained at 25 V. UV−visible spectra were recorded on a Shimadzu Multispec-1500 diode array spectrophotometer at room temperature. Elemental analysis was performed by Yanako CHN corder MT-6. For the measurements of H_2-consumption, a constant pressure gas buret (Taitec Co.) was used at 30 °C. H_2, HD, and D_2 gases were determined by Shimadzu GC-16A {He carrier, 10% $MnCl_2$-alumina 100/120 column (4.0 m × 3.0 mm i.d.) at −196 °C (liquid N_2)} and GC-8A {He carrier, molecular sieve-13X 30/60 column (4.0 m × 3.0 mm i.d.) at 40 °C} equipped with a thermal conductivity detector. NO and NO_2 gases were determined by NO_x gas analyzer (Shimadzu NOA-7000) equipped with a chemiluminescence detector under N_2 atmosphere. The volumes of H_2, NO, and NO_2 were corrected by the pressure and temperature of each experiment.

pH of the Solution. The pH of the solution was adjusted by using 0.01−10 M HNO_3/H_2O and 0.01 M $NaOH/H_2O$ (or by evaporation of the solvent/dilution of the solution). In a pH range of 1−10, the pH of the solution was determined by a pH meter (TOA; HM-5A) equipped with a glass electrode (TOA; GS-5015C). Below pH 1, the pH of the solution was estimated by the concentration of the solution; for example, pH values of 0.1, 1.0, and 10 M HNO_3/H_2O were estimated to be 1, 0, and −1, respectively. Values of pD were corrected by adding 0.4 to the observed values (pD = pH meter reading + 0.4).[11]

Syntheses of $[(Cp^*Ir^{III})_2(\mu\text{-}H)_3]NO_3$ ($\mathbf{2}\cdot NO_3$). The aqua complex $[Cp^*Ir^{III}(H_2O)_3]SO_4$ ($\mathbf{1}\cdot SO_4$, 477 mg, 1.0 mmol) reacts with H_2 (0.1 MPa) in HNO_3/H_2O (100 mL) in the pH range of about 1−4. After being stirred for 4 h at 30 °C, the mixture was concentrated to ca. 10 mL. To the solution was added 10 mL of 5 M HNO_3/H_2O (or 5 M $NaNO_3/H_2O$) giving a yellow powder of $\mathbf{2}\cdot NO_3$, which was collected by filtration, washed with a small amount of ether, and dried in vacuo (yield: 70% based on $\mathbf{1}\cdot SO_4$). ^1H NMR (500 MHz, HNO_3/H_2O at pH 2): δ −15.40 (s, μ-H), 2.08 (s, η^5-$C_5(CH_3)_5$). ^{13}C NMR (HNO_3/H_2O at pH 2): δ 11.09 (s, η^5-$C_5(CH_3)_5$), 86.94 (s, η^5-$C_5(CH_3)_5$). ESI-MS (HNO_3/H_2O at pH 2): *m*/*z* 657.4 {relative intensity (*I*) = 100% in the range of *m*/*z* 100−2000}. UV−vis (HNO_3/H_2O at pH 2): λ_{max} (nm), ϵ (M^{-1} cm^{-1}): 304, 28 000. Anal. Calcd for $C_{20}H_{33}Ir_2NO_3$: C, 33.37; H, 4.62; N, 1.95. Found: C, 33.09; H, 4.55; N, 1.92.

X-ray Crystallographic Analysis. Crystallographic data for $\mathbf{2}\cdot(NO_3)(H_2O)_4$ and **3** have been deposited with the Cambridge Crystallographic Data Center as supplementary publication no. CCDC-157 603 {for $\mathbf{2}\cdot(NO_3)(H_2O)_4$} and 157 604 (for **3**), respectively. Copies of the data can be obtained free of charge on application to CCDC, 12 Union Road, Cambridge CB21EZ, U.K. {fax, (+44)1223-336-033; e-mail, deposit@ccdc.cam.ac.uk}. Measurements were made on a Rigaku/MSC Mercury CCD diffractometer and a Rigaku AFC-7R four-circle diffractometer with graphite monochromated Mo Kα radiation (λ = 0.7107). All calculations were performed using the teXsan crystallographic software package of the Molecular Structure Corp. Crystal data, data collection parameters, structure solution and refinement, atomic coordinates, anisotropic displacement parameters, bond lengths, and bond angles are given in the Supporting Information.

Acknowledgment. Financial support of this research by the Ministry of Education, Science, Sports, and Culture, Japan Society for the Promotion of Science, and Grants-in-Aid for Scientific Research to S.O. (13640568) and Y.W. (11490036 and 11228208) is gratefully acknowledged. We thank Professors K. Isobe (Osaka City University) and S. Fukuzumi (Osaka University) for valuable discussions.

Supporting Information Available: Crystallographic information (PDF). This material is available free of charge via the Internet at http://pubs.acs.org.

JA011846L